

## Linear relation between deuteron matter radius and the scattering length

D. W. L. Sprung, Hua Wu and J. Martorell\*

*Department of Physics, McMaster University, Hamilton, Ontario, Canada L8S 4M1*

(Received 16 April 1990)

We explain the empirical linear relations between the triplet scattering length, or the asymptotic normalization constant, and the deuteron matter radius using the effective range expansion in a manner similar to a recent paper by Bhaduri *et al.* We emphasize the corrections due to the finite force range and to shape dependence. The discrepancy between the experimental values and the empirical line shows the need for a larger value of the wound extension, a parameter which we introduce here. Short-distance nonlocality of the  $n$ - $p$  interaction is a plausible explanation for the discrepancy.

### I. INTRODUCTION

Some time ago we found<sup>1</sup> an empirical linear relation between the deuteron mean square matter radius  $r_m$  and the triplet even effective range  $a_t$ , obeyed by all the “realistic” potential models of the nucleon-nucleon interaction which we had examined. This relation is displayed in Fig. 1. The experimental values of these quantities lie 3 standard deviations off the line. While we did not have a theoretical derivation of the linear relation, it seemed clear that the discrepancy was significant, and pointed to a surprising failure of the nonrelativistic potential models to explain deuteron properties in conjunction with the low-energy scattering data.

Recently, Bhaduri *et al.*<sup>2</sup> have found a partial explanation for this linear relation. They presented an analytic argument, backed up by some specific examples using a variety of simple potential models. Specifically, they obtained

$$\frac{\langle r^2 \rangle}{a_t^2} \approx \frac{1}{8} \left( 1 + \frac{1}{4} x_B^2 + \frac{1}{2} x_B^3 + \dots \right) (1 + 24\eta^2), \quad (1)$$

where  $x_B = \rho/a_t \approx 0.33$  is the ratio of the effective range to the scattering length in the triplet even state; see Eq. (6) below. We have a somewhat simpler derivation of their result, to which we have added the correction for the finite range of the nucleon-nucleon force. This allows us to give a complete explanation for the empirical linear relation. We find that the slope of this line is very sensitive to the “healing function,” and in particular to the “wound extension”  $K$ , which are defined below. We establish that the experimental  $r_m$  and  $a_t$  require a larger value of  $K$  than is obtained from the standard potential models. Recently Kermodé *et al.*<sup>3</sup> have constructed a potential model which incorporates short range nonlocal attraction, which does reproduce the experimental radius, and correspondingly the required large  $K$ . This points to short-distance nonlocality as a plausible explanation for the discrepancy. Such nonlocality arises from coupling of

the nucleon-nucleon channel to exotic components of the deuteron wave function, which may be either isobars or explicit quark degrees of freedom.

### II. ASYMPTOTIC RELATION FOR SQUARED MATTER RADIUS

#### A. $S$ wave only

The important point in Ref. 2 was to use an expansion around  $\rho = 0$ . This is the zero-range approximation, given by a boundary condition at  $r = 0$ ,

$$\left. \frac{u'}{u} \right|_{r=0} = -\alpha. \quad (2)$$

This implies that the scattering length is  $a_t = 1/\alpha$ , while the deuteron wave function is

$$u(r) = A_S e^{-\alpha r} \equiv A_S \bar{u}(r), \quad (3)$$

with

$$\frac{A_S^2}{2\alpha} = 1. \quad (4)$$

The mean square radius is

$$\begin{aligned} \langle r^2 \rangle_0 &= \frac{1}{4} \int_0^\infty A_S^2 \bar{u}^2(r) r^2 dr \\ &= \frac{A_S^2}{16\alpha^3} = \frac{a_t^2}{8} \end{aligned} \quad (5)$$

This is the leading term in their expansion. It reflects the fact that the radius and the scattering length are two measures of the size of the  $n$ - $p$  system at low energy. The scattering length  $a_t$  measures the decay length of the zero-energy wave function, while  $\langle r^2 \rangle$  measures that of the wave function squared. This accounts for one factor of 2. The additional factor of 4 comes because the radius is measured from the center of mass, while  $a_t$  is a separation distance.

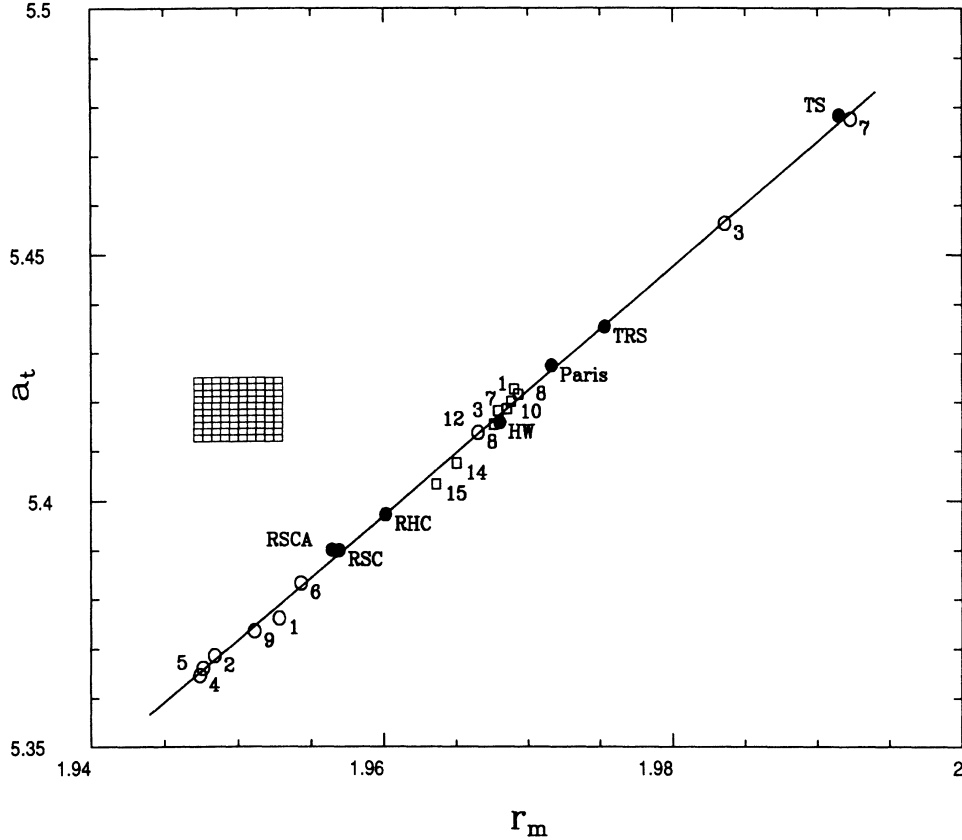


FIG. 1. The empirical linear relation between the scattering length  $a_t$  and deuteron matter radius  $r_m$  as presented in Fig. 6 of Ref. 1. The experimental values with their uncertainties lie in the shaded box which lies about 3 standard deviations off the empirical line.

### B. Coupled $S$ and $D$ waves

In the general case, including tensor forces, one must distinguish between three different effective ranges.

$$k \cot \delta_\alpha \equiv y(k^2) = -\frac{1}{a_t} + \frac{1}{2}\rho_0 k^2 - k^4 \rho_d^3 g(k^2) \quad (6)$$

defines the zero-energy effective range  $\rho_0$ . The phase shift  $\delta_\alpha$  is the Blatt-Biedenharn eigenphase, and the dimensionless function  $g(k^2)$  allows for corrections to the shape-independent approximation as discussed recently in Ref. 4. If instead we expand  $y(k^2)$  around the deuteron pole, one has

$$y(k^2) = -\alpha + \frac{1}{2}\rho_d(k^2 + \alpha^2) + \dots \quad (7)$$

This effective range  $\rho_d$  is the slope of  $y$  at  $k^2 = -\alpha^2$ . A third effective range is the slope  $\rho_m$  of the chord joining  $k^2 = 0$  to  $k^2 = -\alpha^2$ . One has

$$\alpha = \frac{1}{a_t} + \frac{1}{2}\rho_m \alpha^2. \quad (8)$$

In practice, the three effective ranges are not exactly equal, but the differences between them are tiny and give information on the degree of shape dependence in the neutron-proton interaction.<sup>4</sup>

From effective range theory, one has

$$\frac{1}{2}\rho_d = \int_0^\infty H(r) dr, \quad (9)$$

where the "healing function" is defined by

$$H(r) \equiv \bar{u}^2 - \frac{u^2(r) + w^2(r)}{A_S^2(1 + \eta^2)}. \quad (10)$$

Since the deuteron wave function, normalized to unity

$$\int_0^\infty [u^2(r) + w^2(r)] dr = 1$$

has the asymptotic limits

$$u(r) \rightarrow A_S e^{-\alpha r} = A_S \bar{u}(r), \quad (11)$$

$$w(r) \rightarrow A_S \eta \bar{w}(r),$$

with

$$\bar{w}(r) \equiv \left(1 + \frac{3}{z} + \frac{3}{z^2}\right) e^{-z}, \quad z = \alpha r, \quad (12)$$

$H(r)$  will vanish at large distances beyond the centrifugal barrier. But at distances of order 5 fm, where  $w(r)$  is converging towards  $\bar{w}(r)$ , one has  $\bar{w}(r) \approx 6\bar{u}(r)$ , which

contributes a negative tail to the healing function. (See Fig. 2, below.)

Finally, we need the expression for the mean square matter radius of the deuteron, which is

$$\begin{aligned} \langle r^2 \rangle &= \frac{1}{4} \int_0^\infty [u^2(r) + w^2(r)] r^2 dr \\ &= \frac{A_S^2(1 + \eta^2)}{4} \int_0^\infty [\bar{u}^2(r) - H(r)] r^2 dr \\ &\equiv \langle r^2 \rangle_{as} + \langle \delta r^2 \rangle. \end{aligned} \quad (13)$$

Since  $\langle r^2 \rangle_{as}$  depends only on the asymptotic wave function, it will have the same expansion as found in Ref. 2. This is derived as follows. From Eqs. (9)–(11) one obtains

$$\frac{1}{2} \rho_d = \frac{1}{2\alpha} - \frac{1}{A_S^2(1 + \eta^2)},$$

giving

$$A_S^2(1 + \eta^2) = \frac{2\alpha}{(1 - \alpha\rho_d)}. \quad (14)$$

We define our expansion parameter to be  $x_d = \alpha\rho_d$ . Also from Eq. (8) we have

$$\frac{1}{a_t} = \alpha(1 - \frac{1}{2}\alpha\rho_m). \quad (15)$$

This involves  $x_m = \alpha\rho_m \approx x_d$ . Then from Eqs. (13)–(15) one has

$$\langle r^2 \rangle_{as} = \frac{A_S^2(1 + \eta^2)}{16\alpha^3} = \frac{1}{8} \frac{1}{\alpha^2} \frac{1}{(1 - x_d)}, \quad (16)$$

Treating the two effective ranges as equal,

$$\begin{aligned} \frac{\langle r^2 \rangle_{as}}{a_t^2} &= \frac{1}{8} \frac{(1 - x_m/2)^2}{(1 - x_d)} \\ &= \frac{1}{8} \left( 1 + \frac{\frac{1}{4}x^2}{(1 - x)} \right), \end{aligned} \quad (17)$$

where  $x = \alpha\rho \approx 0.4$ . This shows that in the shape-independent approximation, there is no term linear in  $x$  in the expansion, and also that the higher order terms in the expansion essentially double the result of the  $x^2$  term. Bhaduri *et al.* did not give a closed form for the series despite making essentially the same approximations as we have introduced. Their expansion parameter  $x_B$  is related to ours by Eq. 15,

$$x_m(1 - \frac{1}{2}x_m) = \frac{\rho_m}{a_t} \approx x_B. \quad (18)$$

One then sees that the  $x^2$  terms are the same, while the cubic term has coefficient  $\frac{1}{4}$  in our series, and  $\frac{1}{2}$  in theirs, in the shape-independent approximation. Whether one uses  $x_m$  (or  $x_d$ ) instead of  $x_B$  in the expansion is largely a matter of taste, because the three effective ranges differ among themselves only in terms of order  $x^3$  (see below), and  $\alpha\rho$  differs from  $\rho/a_t$  only in order  $x^2$ . In either case the physical basis for the expansion is the weak binding

of the deuteron, which makes  $x < 1$ . We believe that our choice gives the simpler expressions.

Going beyond the shape-independent approximation, from Eqs. (6)–(8) one finds that

$$x_d - x_m = 2x_d^3 \left( \frac{d}{dk^2} [k^2 g(k^2)] \right)_{-\alpha^2} \equiv dx_d^3. \quad (19)$$

Using the estimate  $\rho_d - \rho_m = 0.012 \pm 0.002$  fm, deduced from systematics of potential models,<sup>5</sup> the coefficient  $d$  has the small value 0.046. Nonetheless, we shall see that accurate work requires that we treat  $x_d$  and  $x_m$  as distinct.

### III. HEALING FUNCTION AND WOUND EXTENSION

The correction to the above result, Eq. (17), due to the difference between the exact and asymptotic wave functions, is given by an integral over the healing function, as in Eq. (13). Since  $u(r)$  and  $w(r)$  vanish at the origin,  $H(r)$  is positive at small distances, making the correction to the mean square radius negative.  $H(r)$  is constrained to have its area equal to half the effective range. The simplest model which satisfies the required properties is a linear one:

$$H(r) = \begin{cases} 1 - r/\rho_d, & 0 < r < \rho_d \\ 0, & r > \rho_d. \end{cases} \quad (20)$$

This gives

$$\langle \delta r^2 \rangle = -\frac{1}{8} \frac{1}{\alpha^2} \frac{K x_d^3}{(1 - x_d)} \quad (21)$$

with  $K = \frac{1}{3}$ . In general,

$$K = \frac{4}{\rho_d^3} \int_0^\infty H(r) r^2 dr. \quad (22)$$

We call this parameter the “wound extension,” as it is a dimensionless measure of the radial distribution of the healing function. Since the coefficient of the  $x_B^3$  term in Bhaduri’s expansion [Eq. (1)] was  $\frac{1}{2}$ ,  $K = \frac{1}{3}$  represents a major reduction in its value. Ericson, in his Karlsruhe conference talk<sup>6</sup> used a Hulthén model for the wave function, and found  $K = \frac{5}{9}$ . (There is a misprint in that paper.) Other simple models expressing  $H(r)$  by exponentials give  $K$  ranging from  $\frac{1}{4}$  to 1. It is this finite-force-range correction, then, which is primarily responsible for reducing the mean square matter radius below its asymptotic value. This shows why, in the particular analytic models presented in Ref. 2, the coefficient of the cubic term was always much smaller than  $\frac{1}{2}$ . (In our expansion, the cubic coefficient is  $\frac{1}{4}$ , so the reduction by  $K$  is even more significant.)

For a more realistic estimate of  $\langle \delta r^2 \rangle$ , we use the Paris wave function.<sup>7</sup> Figure 2 is a plot of  $r^2 H(r)$ . The area under  $H(r)$  is by definition  $\frac{1}{2}\rho_d$ , and comes mainly from small  $r$ . When the  $r^2$  weighting is factored in, the contributions from the “core” ( $r < 0.4$  fm), “intermediate,” and “outer” ( $r > 1.4$  fm) regions are about 0.018,

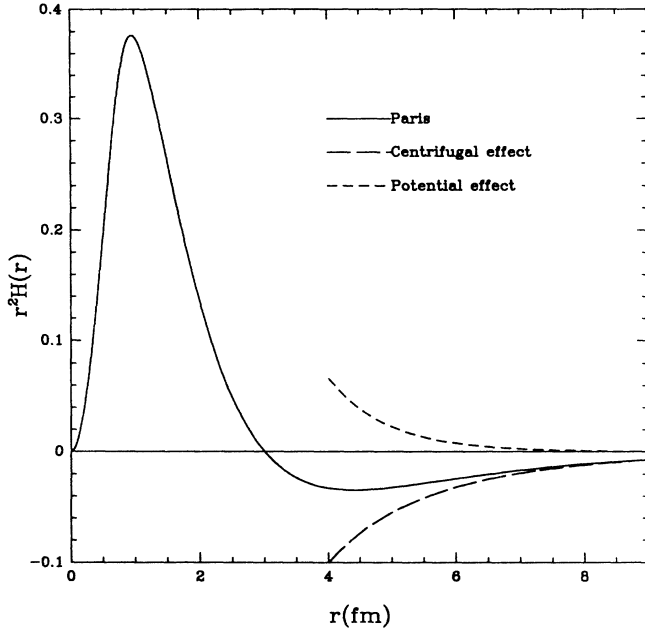


FIG. 2. The “healing function” times  $r^2$  for the Paris wave function. The long-dashed line shows the negative tail due to the centrifugal barrier in the  $D$  state. The short-dashed line is the difference between the full curve and the centrifugal effect, and is due to the slow convergence of the wave function to its asymptotic form, Eq. (3).

0.306, and 0.042, respectively, giving  $K = 0.261$ . That from the outer region is greatly reduced by the negative tail seen in Fig. 2. As we have remarked at Eq. (12), this negative tail is due to  $\bar{w}$  being about six times larger than  $\bar{u}$  when  $r \approx 6$  fm. The long dashed line in Fig. 2 shows this “centrifugal barrier” effect, and corroborates that  $\bar{w}$  is responsible. It is this negative tail which was taken account of in Ref. 2, by an overall factor of  $1 + 24\eta^2$  on  $\langle r^2 \rangle_{as}$ , but the large negative correction due to the positive peak of  $H(r)$  was not included. We think it is more appropriate to include both these corrections in the  $x^3$  term as we have done here. (But see below for further discussion.)

The trial wave functions used by Butler and Sprung<sup>8</sup> give a somewhat broader healing function; that corresponding to their parameter set “a” is shown in Fig. 3. The main peak is displaced outwards by 0.5 fm and the negative tail begins about 1 fm later than in Fig. 2. In both figures, the short-dashed line denoted “potential effect” shows what one would have in the absence of the centrifugal barrier on the  $D$  state. The contributions to the integral from the “core,” “intermediate,” and “outer” regions from Fig. 3 are 0.017, 0.300, and 0.339, respectively, giving a  $K = 0.472$  for this wave function. This shows the great sensitivity of  $K$  to small differences in the wave function. It should be noted that this wave function gives a root mean square radius 1.955 fm, very close to the experimental value.<sup>1</sup>

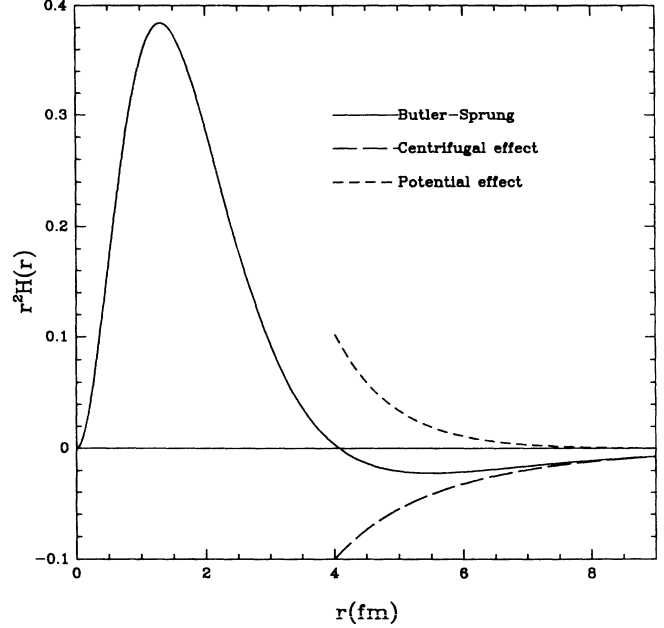


FIG. 3. Same as Fig. 2 but for the Butler-Sprung wave function.

Given that the healing function has an area of  $\frac{1}{2}\rho_d$ , the only way to increase  $\langle \delta r^2 \rangle$  is to move some of the area out to larger radii. Supersoft core potentials should tend to do this, as they have softer but wider repulsive cores. But in practice no significant effect is seen. Bhaduri *et al.* noted that their separable force models did tend to have a negative net coefficient of the  $x^3$  term. This would be the result of a large  $K$  value. Indeed, Kermode *et al.*<sup>3</sup> have recently constructed a model similar to the Reid hard core (RHC) potential, but with an increased short range local repulsion balanced by a short range separable attraction, which has a deuteron matter radius of 1.95 fm. Their  $H(r)$  does show a significant shift of the peak in  $r^2H(r)$  outwards by about 1 fm, giving a much larger  $K$  than for the purely local RHC potential. In an earlier paper we argued<sup>4</sup> that one-pion exchange potential dominance plus experimental measurements of a number of deuteron properties impose strong constraints on the deuteron wave function outside 1.4 fm. Our method of integrating inwards from infinity through the potential relied upon the potential being local outside one-pion Compton wavelength. The potential of Kermode *et al.* would appear to violate these assumptions. In order to shift the peak of  $r^2H(r)$  outwards, they introduce an oscillation into  $u(r)$  which can only be obtained with non-local forces. (For a local potential, the points of inflection coincide with the nodes.)

#### IV. LINEAR RELATIONS

Combining Eqs. (17) and (21), we have

$$\begin{aligned} \frac{\langle r^2 \rangle}{a_t^2} &= \frac{1}{8} \frac{(1 - x_m/2)^2}{(1 - x_d)} (1 - K x_d^3) \\ &= \frac{1}{8} \left( 1 + \frac{\frac{1}{4} x_m^2 + x_d - x_m}{1 - x_d} \right) (1 - K x_d^3). \end{aligned} \quad (23)$$

This is almost our final result. For any potential model, the calculated values of the “wound extension” Eq. (22), radius, and scattering length, will precisely satisfy Eq. (23). However, in order to understand the slope of the empirical  $r_m$  vs  $a_t$  line, we must consider a further refinement to the definition of the parameter  $K$ . In the asymptotic region beyond about 5 fm, the “healing function”  $H(r)$  is negative. We call this the “centrifugal” contribution. From Eqs. (10)–(13) we have

$$H_{ce}(r) = -\frac{\eta^2}{1 + \eta^2} e^{-2z} \left[ \left( 1 + \frac{3}{z} + \frac{3}{z^2} \right)^2 - 1 \right]. \quad (24)$$

This should be valid for  $z > z_0 \approx 1$ , where  $z = \alpha r$ . Integrating, we find

$$\delta K_{ce} x_d^3 \approx -\frac{\eta^2}{1 + \eta^2} e^{-2z_0} (12z_0 + 36 + 36/z_0). \quad (25)$$

The numerical value is certainly sensitive to the cutoff point, but for  $z_0 = 1$ , we have  $-\delta K_{ce} x_d^3 = 11.4\eta^2$ . If one wishes to extend the integration in to the origin, one must drop the most singular piece of Eq. (12), which leads to the result,  $24\eta^2$ , of Bhaduri *et al.*<sup>2</sup> So we agree that a part of the finite-force-range correction is sensitive to  $\eta^2$ , rather than  $x_d^3$ , but only about half the amount proposed earlier. The remaining part of  $K$  which does scale with  $x_d^3$  has to be larger to compensate. The last factor in Eq. (23) should be replaced by

$$(1 - K x_d^3) = (1 - K_p x_d^3 + C\eta^2). \quad (26)$$

We computed  $K$  for a large selection of well-known potential models, finding  $K$  values in the range  $0.19 < K < 0.27$ , as shown in Table I. The bulk of the dependence on  $x_d$  could be accounted for by Eq. (26). By choosing  $C = 14$  [corresponding to  $z_0 = 0.91$  in Eq. (25)], we found the least variance in the value of  $K_p$ , giving the average value  $K_p = 0.395 \pm 0.007$ . This agrees well with the estimate given above. [We omitted the Reid Soft Core (RSC) and its alternate (RSCA) potentials from the average, because they have shape-dependent terms quite different from the other models, as seen in Fig. 1 of Ref. 5.] Taking the square root of Eq. (23) gives

$$\frac{r_m}{a_t} = \frac{1}{\sqrt{8}} \frac{(1 - x_m/2)}{\sqrt{(1 - x_d)}} \sqrt{1 - K_p x_d^3 + C\eta^2}. \quad (27)$$

When  $a_t$  varies,  $x$  also varies. The empirical straight line in Fig. 1 was only observed<sup>1</sup> over a range of variation in  $a_t$  of about 5%, so it should be adequate to examine only the first derivative. Because the binding energy of the deuteron is essentially the same for all empirical potential models, we can use Eq. (15) to establish that

$$\left. \frac{\partial x_m}{\partial a_t} \right|_{\alpha} = \frac{2}{\alpha a_t^2}. \quad (28)$$

Since  $x_d$  occurs in two places in Eq. (27), we need its derivative as well. According to Fig. 1 of Ref. 5, the two derivatives differ by a nearly constant factor  $f \approx 0.89$ . This leads to

$$\left. \frac{\partial r_m}{\partial a_t} \right|_{\alpha} = \frac{r_m}{a_t} \left\{ 1 + \frac{1}{\alpha a_t} \left[ \frac{f}{(1 - x_d)} - \frac{1}{(1 - x_m/2)} - \frac{3fK_p x_d^2}{(1 - K_p x_d^3 + C\eta^2)} \right] \right\}. \quad (29)$$

The term in square brackets represents the correction to the slope due to the variation of  $x$ . Without it, the slope of the  $a_t - r_m$  line [the inverse of Eq. (29)] would differ by only 1% or 2% from the value  $\sqrt{8}$ . With it, the slope is lower by 10–20%, depending on the value of  $K_p$ . The terms linear in  $x$  give a 30% reduction, but this is moderated substantially by the term involving  $K_p$ . From Fig. 1, one sees that the empirical slope is 2.55, about 10% smaller. Using Eq. (15), we can rewrite Eq. (29) in the form

TABLE I. Values of  $x_d$ ,  $\eta$ , and integral  $K$  [Eq. (22)] for various well-known potential models.  $K_p$  is computed for each model taking  $C = 14$ . The mean value of  $K_p$  is  $0.395 \pm 0.007$ .

Potential	$x_d$	$\eta$	$K$	$K_p$
GK4	0.3944	0.026 77	0.2299	0.3934
GK5	0.3949	0.026 62	0.2386	0.3997
GK2	0.3958	0.026 93	0.2454	0.4091
GK9	0.3972	0.026 70	0.2379	0.3972
GK1	0.3977	0.027 13	0.2179	0.3818
RSC	0.3988	0.026 22	0.1918	0.3435
RSCA	0.3990	0.025 96	0.2005	0.3490
GK6	0.3997	0.026 76	0.2461	0.4031
RHC	0.4028	0.025 90	0.2325	0.3763
FL15	0.4046	0.027 23	0.2361	0.3928
FL14	0.4062	0.027 02	0.2418	0.3943
FL13	0.4074	0.026 86	0.2458	0.3952
GK8	0.4076	0.026 54	0.2444	0.3900
FL12	0.4083	0.026 67	0.2502	0.3965
FL11	0.4083	0.026 63	0.2507	0.3965
HW	0.4088	0.026 42	0.2469	0.3900
FL10	0.4090	0.026 49	0.2543	0.3979
FL9	0.4090	0.026 48	0.2546	0.3981
FL7	0.4095	0.026 28	0.2596	0.4004
FL4	0.4097	0.026 19	0.2614	0.4010
FL5	0.4097	0.026 20	0.2614	0.4011
FL6	0.4097	0.026 21	0.2613	0.4012
FL8	0.4097	0.026 28	0.2593	0.3999
FL1	0.4099	0.025 81	0.2707	0.4061
FL2	0.4099	0.026 05	0.2649	0.4028
FL3	0.4099	0.026 09	0.2650	0.4033
PARIS	0.4113	0.026 08	0.2615	0.3983
TRS	0.4136	0.026 22	0.2566	0.3926
GK3	0.4197	0.025 95	0.2646	0.3922
TS	0.4245	0.026 22	0.2716	0.3974
GK7	0.4252	0.025 64	0.2667	0.3864

$$\left. \frac{\partial r_m}{\partial a_t} \right|_{\alpha} = \frac{r_m}{a_t} \left\{ (1 - x_m/2)f \times \left[ \frac{1}{(1 - x_d)} - \frac{3K_p x_d^2}{(1 - K_p x_d^3 + C\eta^2)} \right] \right\}. \quad (30)$$

With the values of  $K_p$  and  $C$  fitted above, we find excellent agreement with the empirical slope of the  $a_t - r_m$  line.

What we conclude, then, is that the zero-range limit would give a slope of  $\sqrt{8}$  and a strictly linear relationship. The finite-range correction removes the linearity and decreases the slope in the region where the empirical potentials have been fitted. The exact amount of reduction is sensitive to the finite-force-range correction, which is an off-shell effect. The slope observed for the "realistic" potential models implies that  $K_p \approx 0.4$ , rather larger than the total  $K$  value for the Paris potential, and the difference is due to the "centrifugal" contribution. The  $D$  state is thus seen to make the asymptotic radius a better approximation to the complete radius, since it reduces the finite-size correction.

Finally, we remark on the second linear relation discussed in Ref. 1, that between the asymptotic normalization constant  $A_S$  and the matter radius. From Eqs. (16) and (21) one can write

$$\langle r^2 \rangle = \frac{A_S^2(1 + \eta^2)}{16\alpha^3} (1 - K_p x_d^3 + C\eta^2). \quad (31)$$

Taking the square root, one has  $A_S \approx 0.45r_m$ , in good agreement with points on the line in Fig. 7 of Ref. 1. Taking into account the dependence of  $A_S$  on  $x_d$ , we find for the slope

$$\left. \frac{\partial A_S}{\partial r_m} \right|_{\alpha} = \frac{A_S}{r_m} \left( 1 - \frac{3K_p x_d^2(1 - x_d)}{(1 - K_p x_d^3 + C\eta^2)} \right)^{-1}, \quad (32)$$

In the figure, the slope is about 17% greater than the ratio, and this is well reproduced with  $K_p = 0.395$  as deduced above.

The empirical linear relations obeyed by the realistic potential models appear then to have their explanation in the weak binding of the deuteron relative to the range of the nuclear force. The matter radius is close to its asymptotic value, the deviation depending sensitively on the details of the healing function. To reduce the radius to its experimental value,<sup>1</sup> without altering  $a_t$ , requires a substantial  $K$  value. The peak in  $r^2 H(r)$  must be moved out

relative to its location for the Paris potential. Kermode *et al.* have managed to do this by employing a separable attraction at small distances. Their  $u(r)$  has a lower and broader maximum just outside the core radius than for a purely local interaction. This may be the clearest evidence for a nonlocal component of the nucleon-nucleon interaction. The physical basis for this nonlocality lies in coupling of the  $NN$  channel to exotic components of the deuteron wave function, but whether these are isobaric components or quark substructure of the nucleon is not revealed by this evidence. In any case, the fact<sup>1</sup> that the experimental radius and scattering length do not lie on the empirical line requires a larger  $K$  than is provided by the usual local potential models, closer to the value 0.47 given by the Butler-Sprung wave function.

## V. CONCLUSION

In summary, we have improved upon, and simplified the derivation of, the expansion of Bhaduri *et al.*<sup>2</sup> for the asymptotic radius. We have emphasized that the finite-range correction alters this expansion in order  $x^3$ , as already pointed out by Ericson.<sup>6</sup> We have taken into account the differences among the effective ranges and shown that the centrifugal barrier in the  $D$  state reduces the correction to the asymptotic radius over what would be expected in a purely  $S$ -state model. Finally, we have shown that when one takes into account the variation of  $x_d$  with respect to  $a_t$ , the expansion can indeed explain the empirical linear relations found by us some time ago. We emphasize that the developments in this paper depend only on analyticity of the scattering matrix and the existence of the healing function, but not on the use of the Schrödinger equation. Hence, the conclusion that the data require a larger value of the wound extension is independent of the model which led us to discover the linear relations among these observables.

## ACKNOWLEDGMENTS

Support from Natural Sciences and Engineering Research Council under operating Grant A-3198, and from Dirección General de Investigaciones Científicas y Tecnológicas under Grants PS-88-0045 and PB-87-0311, is gratefully acknowledged. We also thank Dr. Van Dijk for informing us about his wave functions, and Dr. Bhaduri for an advance copy of his article.

\*Permanent address: Dept. de Estructura i Constituents de la Materia, Universitat Barcelona, 08028 Spain.

<sup>1</sup>S. Klarsfeld, J. Martorell, J.A. Oteo, M. Nishimura, and D.W.L. Sprung, Nucl. Phys. **A456**, 373 (1986).

<sup>2</sup>R.K. Bhaduri, W. Leidemann, G. Orlandini, and E.L. Tomasiak, Phys. Rev. C (to be published).

<sup>3</sup>M.W. Kermode, M.M. Mustafa, S. Moszkowski, and W. Van Dijk, private communication.

<sup>4</sup>S. Klarsfeld, J.A. Oteo, and D.W.L. Sprung, J. Phys. G

**15**, 849 (1989); **15**, 1627 (Corrigendum) (1989).

<sup>5</sup>S. Klarsfeld, J. Martorell, and D.W.L. Sprung, J. Phys. G **10**, 165 (1984).

<sup>6</sup>T.E.O. Ericson, Nucl. Phys. **A416**, 281 (1984).

<sup>7</sup>M. Lacombe, B. Loiseau, R. Vinh Mau, J. Côté, P. Pirès, and R. de Tournell, Phys. Lett. **101B**, 139 (1981).

<sup>8</sup>M.N. Butler and D.W.L. Sprung, Can. J. Phys. **62**, 65 (1984).